MedChemComm

Accepted Manuscript

This article can be cited before page numbers have been issued, to do this please use: P. RICHARDSON, V. L. Mariin, S. L. Koeniger, A. Baranczak, J. L. Wilsbacher, P. J. Kovar, P. E. Bacon-Trusk, M. Cheng, T. A. Hopkins, S. T. Haman and A. Vasudevan, *Med. Chem. Commun.*, 2019, DOI: 10.1039/C8MD00412A.

ROYAL SOCIETY OF CHEMISTRY

rsc.li/medchemcomm

View Article Online
DOI: 10.1039/C8MD00412A

MedChemComm

PAPER

Controlling Cellular Distribution of Drugs with Permeability Modifying Moieties

Received 00th January 20xx,
Accepted 00th January 20xx

DOI: 10.1039/x0xx00000x

www.rsc.org/

Paul L. Richardson,*[a] Violeta L. Marin,[a] Stormy L. Koeniger,[a] Aleksandra Baranczak,[a] Julie L. Wilsbacher,[b] Peter J. Kovar,[b] Patricia E. Bacon-Trusk,[b] Min Cheng,[b] Todd A. Hopkins,[b] Sandra T. Haman,[b] and Anil Vasudevan[a]

Phenotypic screening provides compounds with very limited target cellular localization data. In order to select the most appropriate target identification methods, determining if a compound acts at the cell-surface or intracellularly can be very valuable. In addition, controlling cell-permeability of targeted therapeutics such as antibody-drug conjugates (ADCs) and targeted nanoparticle formulations can reduce toxicity from extracellular release of drug in undesired tissues or direct activity in bystander cells. By incorporating highly polar, anionic moieties via short polyethylene glycol linkers into compounds with known intracellular, and cell-surface targets we have been able to correlate the cellular activity of compounds with their subcellular site of action. For compounds with nuclear (Brd, PARP) or cytosolic (dasatinib, NAMPT) targets, addition of the permeability modifying group (small sulfonic acid, polycarboxylic acid, or a polysulfonated fluorescent dye) results in near complete loss of biological activity in cell-based assays. For cell-surface targets (H_3, $5HT_{1A}$, β_2AR) significant activity was maintained for all conjugates, but the results were more nuanced in that the modifiers impacted binding/activity of the resulting conjugates. Taken together, these results demonstrate that small anionic compounds can be used to control cell-permeability independent of on-target activity and should find utility in guiding target deconvolution studies and controlling drug distribution of targeted therapeutics.

Introduction

The pharmaceutical industry faces well-documented research productivity challenges with the discovery and development of therapeutic agents being estimated to cost as much as $2.87 billion per new molecular entity (NME) approved.[1] In the case of clinical candidates identified via target-based screening, attrition due to lack of efficacy resulting from poorly understood human target validation is a significant issue.[2] In order to enhance the probability of clinical success there is renewed interest in target agnostic phenotypic screening approaches. While phenotypic screening more closely aligns the drug treatment with the desired outcome, it presents alternative medicinal chemistry challenges related to the inherent complications of biological screening assays (e.g. off-target effects, differential compound distribution) and low-throughput for *in vivo* screening assays if used in the early stages of drug discovery.[3] Therefore, there is a strong incentive to identify direct targets from phenotypic screening hits as early in the drug discovery funnel as possible so that target-based high-throughput approaches can be used in the hit-to-lead and lead-optimization stages.[4] The preferred choice of target deconvolution method is often dependent on the type, and quantity of target present in the target cells or tissue. The most commonly applied chemoproteomic methods rely on photo-affinity labelling (PAL) or direct affinity pulldowns.[5] Although PAL is equally applicable to membrane and cytosolic targets,[6] as well as for low-affinity targets direct from phenotypic screens, PAL is challenging due to the usually low cross-linking efficiency, high non-specific crosslinking to false targets and the poor relative quantitation of crosslinking between different targets.[7] Alternatively, small-molecule chemoproteomic target identification by affinity precipitation/mass-spectrometry (MS) is most successful with highly expressed soluble targets. In addition to low abundance, multipass membrane proteins tend to be denatured by the lysis methods used to free potential protein targets from other cellular components and contain hydrophobic sequences with poor MS sensitivity.[8] This results in a general loss of intramembrane target data even though such targets represent a large proportion of targets for approved therapeutics. Alternatively, methods appropriate for the identification of cell-surface membrane proteins such as ligand-directed acyl imidazole[9] or GlycoCLICK require non-permeable reagents attached to the test compounds that result in poor identification of intracellular targets.[10] Because of the mutually exclusive nature of these methods of target identification we sought an efficient means of determining whether compounds had cell-surface or intracellular targets

[a] *Drug Discovery Science and Technologies, 1 North Waukegan Rd, North Chicago, IL 60064, USA. E-mail: paul.l.richardson@abbvie.com.*
[b] *Discovery Oncology, AbbVie Inc.*
[c] *These authors contributed equally to development of this manuscript*
† The authors declare no competing interests
‡ Electronic Supplementary Information (ESI) available: Synthetic experimental details and extended assay results for select compounds. See DOI: 10.1039/x0xx00000x

driving the phenotypic response. In addition, for cell-surface targets, we wanted to determine whether a crosslinking moiety such as a reactive acylimidazole, or strained alkyne responsive group could be linked to the test compound and still reach the cell-surface in order to crosslink with extracellular domains of potential targets.

There are many ways of assuring compounds remain cell-impermeable, including attaching macromolecules such as serum albumin[11] and polymers such as dextran, PEG[12] or dendrimers,[13] however, maintaining target-based functional activity of such conjugates or complexes is unpredictable. In other cases highly anionic fluorescent dyes have been employed, but these dyes tend to be large molecules with localization/distribution properties of their own.[14,15] In addition, although dye conjugates are useful for imaging applications their fluorescence properties interfere with the ability to run fluorescence-based screening assays to assess independent target engagement. We have performed comprehensive studies (linking strategies, binding and cell-based biological activity measurements, and for a subset of targets (Brd, dasatinib, H_3 receptor), cell-associated unbound drug accumulation ratios - Kp_{uu}[16]) of small moieties that can be used to modify cell permeability of compounds and triage target identification methods. By selecting ligands with a range of nuclear, cytosolic and cell-surface targets with which to test permeability modifier strategies we were able to perform proof of concept studies and provide tools to apply to our own target deconvolution and cell-disposition efforts (Fig. 1).

Results and discussion

General design of permeability modified compounds

Ligands for these experiments were chosen based on their known target subcellular localization patterns and included nuclear ((+)-JQ-1 **1** - Brd2, 3, olaparib **2** – PARP1), cytosolic (dasatinib **3** - kinases, FK866 **4** - NAMPT), and cell-surface (**5** - H_3 receptor, alprenolol **6** - $5HT_{1A}$ and β_2AR) targets (Table 1). Structural data or structure-activity information was used to guide the addition of the required linkers and permeability moieties such that direct on-target binding was minimally impacted in most cases. Where information to guide design was lacking, multiple vectors for addition of the linkers were chosen. When possible, direct on- target activity was explicitly measured, along with PAMPA permeability[17] and cell-based assays specifically sensitive to each modified compound. Short, discrete polyethylene glycol (dPEG) linkers with *tert*-butyloxycarbonyl (Boc) protected amine head groups to couple the ligands to the permeability modifiers were chosen to minimize impact on physico-chemical properties of the conjugates relative to the parent drugs (Fig. 2). Although higher molecular weight PEG is known to prevent cellular uptake, such short linkers have been used for linking reporters to ligands with minimal disruption of permeability and target-binding properties of the whole conjugate while maintaining aqueous solubility.[18] Removal of the Boc group provided a relatively orthogonal reactive primary amine with which to attach the permeability moieties via acylation chemistry. The permeability moieties chosen included a polysulfonated cyanine fluorophore (SCD), a small sulfonic acid containing group (sulfoacetic acid, SAA), and a symmetric polycarboxylate (4-carbonyl-cyclobutane-1,2,3-tricarboxylic acid, CCT) (Fig. 2) to give the test compounds detailed (Fig. 3). Detailed synthetic procedures and characterization of resulting modified compounds are described in the supplementary information.

Table 1 Test compounds, targets and localization.

Compound		Target(s)	Localization
((+)-JQ-1	**1**	BRD2,3,4; BRDT	Nucleus
olaparib	**2**	PARP1, PARP2	Nucleus
dasatinib	**3**	kinases	Cytoplasm
FK866	**4**	NAMPT	Cytoplasm
	5	H_3 receptor	Cell surface
alprenolol	**6**	$5HT_{1A}$ and β_2AR	Cell surface

Design, synthesis and assay results for nuclear targets

The anti-inflammatory/anti-cancer thienodiazepines (Fig. 3, Table 2) derivatives, MS417 and (+)-JQ-1 bind non-selectively to the bromodomains of several BET-family proteins including BRD2, BRD3, BRD4 and BRDT.[19,20] It had been previously shown that the ester of (+)-JQ-1 could be converted to a PEG-linked amide while maintaining binding to BET-family targets.[21] The $dPEG_2$-NH-modified thienodiazepines were prepared directly from (+)-JQ-1. The products were assayed for binding to the BRD2, BRD3 and BRD4 bromodomains using a TR-FRET assay as previously described.[22] Likewise, the cellular activity was measured using two cell-based assay systems: BRD4 in-cell target engagement was shown using an engineered H1299-derived luciferase reporter assay system, and functional BRD4 inhibition was shown in a sensitive breast cancer cell-line MX-1 in a 3-day proliferation assay via CellTiter-Glo (Promega).[22] Finally, the ratio of compound in cells relative to the compound concentration in media (Kp) and cellular unbound drug accumulation ratio (Kp_{uu}) were determined (Table 2, Table S2).[16] Addition of the $dPEG_2$-NHBoc group 1a has a consistent <5-fold impact on binding to BRD2, BRD3, or BRD4 and also a modest impact on either cell-based assay showing that addition of the linker is near SAR-neutral and that the $dPEG_2$-NHBoc minimally affects cellular uptake or in-cell target engagement. Direct PAMPA assay results also show minimal changes in membrane permeability from 2.24 to 6.22 x 10^{-6} cm/s or changes in Kp_{uu} (1, 0.138; 1a, 0.168). Removal of the Boc group provided 1b that maintained binding to the bromodomains, but lost much cellular activity (>15-fold) in each cell-based assay and decreased PAMPA permeability to 0.015 10^{-6} cm/s and ~2-fold loss in Kp_{uu} to 0.0695. Addition of the SCD modifier 1c was not tolerated in the binding assays and resulted in complete abrogation of cell-based activity. The smaller CCT group 1e also consistently impacted bromodomain binding ~20-50 fold, whereas the smaller SAA moiety 1d had <5-fold impact on

target binding. However, both SAA and CCT completely prevented cellular activity in both assays. In all cases there was a larger drop in Kpuu (1c, 0.0064; 1d, 0.0219; 1e, 0.0359) It is unknown if a longer PEG-linker would have maintained binding of the CCT or SCD modified (+)-JQ-1 to the bromodomains, but given the impact longer PEG groups have on cellular permeability, and consistent with our goals of finding permeability modifiers for compounds of unknown mechanism, SAA appears to provide permeability modification of (+)-JQ-1 while minimizing effects on target binding.

Olaparib 2, an approved cancer therapeutic, inhibits the nucleus localized DNA repair enzymes poly (ADP-ribose) polymerase-1 and -2 (PARP) at very high affinity.[23] Replacement of the cyclopropylcarbonyl group with a linker and fluorophore maintains on-target binding.[24] Starting from des-cyclopropylcarbonyl olaparib we prepared the permeability modified derivatives 2a-e as shown in the supplementary material. These probes were tested via TR-FRET PARP1 ligand-displacement assay and CellTiter-Glo-based cell-viability assays in insensitive (DLD1) and sensitive (DLD1 *BRCA2*$^{-/-}$) cell-lines as previously described (Table 3).[25] The PAMPA permeability of olaparib itself was good, 3.37 x 10^{-6} cm/s, but most of the modified derivatives were significantly less permeable with most of the derivatives giving no measureable values (NV). The addition of the dPEG$_2$-NHBoc 2a, Boc-removal 2b and even SCD addition 2c had only modest effects on PARP1 binding, however SAA 2d and CCT 2e adduction impacted direct binding substantially with a >10-fold and >50-fold loss in TR-FRET affinity respectively. Also, from the cell proliferation data it appears that the PARP inhibition sensitive cell-activity correlates very closely with direct target binding values, with very little correlation with any permeability modification by the anionic head group. However, the limited dynamic range of BRCA2$^{-/-}$ modified DLD1 cell-line and/or the extremely high binding affinity of the compounds for PARP1 may be masking any underlying permeability effects for this particular target.

Design, synthesis and assay results for cytosolic targets

Dasatinib 3 is a marketed drug for the treatment of chronic myelogenous leukemia and Philadelphia chromosome-positive acute lymphoblastic leukemia.[26] Beyond the primary Bcr-Abl and Src family tyrosine kinases, dasatinib has many additional molecular targets.[27,28] Previously described modified versions of dasatinib guided the design of permeability modified probes that maintain binding to many targets involved in biological activity.[27,29] To des-ethoxy dasatinib 3f, prepared as described,[30] was added the dPEG$_2$-NHBoc linker via alkylation chemistry to give the desired conjugate 3a which was partially converted to the remaining probes as shown in supplementary material. These were tested in an *in vitro* TR-FRET kinome screening panel[31] using methods generally described[32] with data shown (Table 4, Table S1, Fig. S1). For several of the tested kinases, the SCD fluorescence interfered with the TR-FRET binding assay therefore binding of SCD conjugate 3c to the primary kinase targets of dasatinib were tested in an activity assay (Eurofins DiscoveRx Kinomescan).[33,34] For the primary (Abl, Src) and high-affinity secondary targets of dasatinib (K_i < 10 nM: BTK, CSF1R, DDR1, Fyn, Lck, PDGFRA V561D, PDGFRB, RIPK2, SlK1, TNK2; Table S1) the binding affinity was maintained within 10-fold of dasatinib itself. For four targets (DDR1, RIPK2, SIK1, TNK2) the SCD probe 3c was >10-fold weaker than dasatinib. PAMPA permeability for all but dasatinib (3, 1.49 x 10^{-6} cm/s) itself was significantly reduced (<0.1 x 10^{-6} cm/s), even for the normally permeable dPEG$_2$-NHBoc derivative (3a, 0.056 x 10^{-6} cm/s), but was reduced to NV for 3c. Likewise, the Kp_{uu} values showed little change on the addition of the dPEG2-NHBoc linker (1, 0.712; 1a, 0.654), but dropped significantly with removal of the Boc (1c, 0.0177) and with the anionic groups (1c, 00055; 1d, 0.0061; 1e, 0.0196). Not surprisingly, the order of Kp_{uu} values closely paralleled the cLogP values (Table 4). In order to evaluate the functional consequences of the modifications, the dasatinib sensitive K562 cell-line was incubated with each derivative and cell-viability measured via CellTiter-Glo. In this assay, the weakly permeable Boc protected compound 3a was only 2.6-fold less active than dasatinib, but all other derivatives were >40-fold less active showing the functional consequences of the permeability modifiers against this cytosolic target.

Nicotinamide phosphoribosyltransferase (NAMPT) is a primarily cytosolic protein and potential oncology treatment target because of its key role in maintaining cellular NAD+ levels via salvage synthesis.[35] Recently, several NAMPT inhibitor series have been described[36] including our own isoindoline urea series which have shown target-specific killing of cancer cells.[37] For NAMPT we designed our probes based on the known NAMPT inhibitor FK866 **4** modified with an aminomethyl functional group **4f**[38] prepared from the truncated precursor.[39] Acylation with the dPEG$_2$-NHBoc linker gave the Boc protected intermediate **4a** which was deprotected with TFA to give the free amine **4b**. Addition of the modifying groups was accomplished via acylation **4c-e** (Fig. 3). Measured PAMPA permeability of FK866 was quite high (**4**, 39.5 x 10^{-6} cm/s), but decreased significantly with addition ofthe aminomethyl group (**4f**, 0.09 x 10^{-6} cm/s), rebounded somewhat with the dPEG$_2$-NHBoc (**4a**, 1.2 x 10^{-6} cm/s) and became unmeasureable when the modifiers were added (**4c-4e**, NV). The probes were screened via a TR-FRET ligand displacement assay (Table 5) with the binding affinity of the probes improved by the presence of the NAMPT cofactor 5-phosphoribosyl-1-pyrophosphate (+PRPP versus -PRPP) as expected for this compound series.[37] Activity in the binding assay was impacted <3-fold for the dPEG$_2$-NHBoc compound **4a**, but then decreased with addition of SCD (**4c**, 23.5-fold, -PRPP; 6.5-fold, +PRPP), SAA (**4d**, 47.5-fold, -PRPP; 39.5-fold, +PRPP) or CCT (**4e**, 59.8-fold, -PRPP; 29.5-fold, +PRPP). Except for SCD, the cell-based data was even more striking in the NAMPT-inhibitor sensitive PC3 cell-line. Both SAA **4d** and CCT

View Article Online DOI: 10.1039/C8MD00413A

4e caused complete loss of cell-killing activity as determined by CellTiter-Glo assay,[40] but **4c** maintained cell-killing generally in-line with the loss of binding affinity and not clearly related to permeability. As expected, the non-permeability modifier compounds **4f**, **4a** and **4b** maintained some cell-killing activity. The smaller anionic groups SAA and CCT appear to be more consistent in preventing cellular uptake and killing of NAMPT inhibitor sensitive PC3 cells.

Design, synthesis and binding results for cell-surface targets

There are presently four known histamine-responsive G-protein coupled receptor subtypes (H_1, H_2, H_3, H_4),[41] of which two are well-established therapeutic targets (H_1 – allergic rhinitis and H_2 – gastric acid secretion).[42] More recent work has attempted to target the H_3 receptor resulting in the discovery of several very potent antagonists, including a series of quinolone H_3 inverse-agonists used as the basis of modified probes here.[43] Previous work showing that pyrazole nitrogen linked $dPEG_2$ versions of quinolone H_3 receptor ligands **5** maintained high affinity for the full-length human H_3 receptor[10] allowed the design of the permeability-modified series **5a-e** (Fig. 3). Although all the probes maintained high affinity (<30 nM) K_i for the human H_3 receptor as determined by CEREP agonist ligand displacement assay there was significant variability in relative affinity depending on the identity of the modifier, but much less variability in functional readouts with the exception of $dPEG_2$-NH_2 **5b**, which showed a 50-fold loss in activity (Table 6). Relative to the original ligand **5**, addition of the $dPEG_2$-NHBoc **5a** caused a 33-fold loss in binding which was restored on removal of the Boc group **5b**. The permeability modifiers also impacted binding with CCT **5e** causing a >50-fold binding loss while the impact of SAA **5d** (12.4-fold) and SCD **5c** (4.2-fold) were more modest. As expected for this series of compounds based on an antagonist compound, they were all inactive in the functional agonist assay except the dye-labeled **5c** (88 nM EC50). For this series of H_3 ligands, preventing uptake into cells via permeability modifiers had quantitative, but not qualitative impact on binding to the cell-surface receptor highlighting the utility of the modifiers to verify cell-surface target location.

Alprenolol **6** is a high-affinity non-selective β_2-adrenergic receptor (β_2AR)[44] and serotonin receptor (5-HT_{1A}, 5-HT_{1b}) antagonist.[45] Sufficient SAR and target structural information was available to design linked, modified versions of alprenolol that were anticipated to maintain on-target affinity dependent on linker position and linker length.[46,47] Adaptation of previous work demonstrating that alprenolol could be attached to a thiol modified affinity resin via an ene-reaction to purify β_2AR[46] led to the design of an ester modified alprenolol **6.1f** which was synthesized using a photocatalyzed thiol-ene reaction on the LOPHTOR flow instrument.[48,49] Hydrolysis of the ester and addition of the $dPEG_2$-NHBoc linker via amidation of the resulting carboxylic acid allowed the subsequent production of the permeability modified series as described for the other probes **6.1a-e**. Consistent with previous probes, but less important for cell-surface alprenolol targets, PAMPA permeability for alprenolol (**6**, 10.9 x 10^{-6} cm/s) decreased to <0.1 x 10^{-6} cm/s for **6.1a-e**. Ligand binding to 5-HT_{1A} was modestly affected by addition of the thioether ester **6.1f**, ~3-fold). Addition of $dPEG_2$-NHBoc **6.1a** had minimal additional binding effects but addition of the permeability modifiers impacted binding (**6.1c**, 18.9-fold; **6.1d**, 15.2-fold; **6.1e**, 35.2 fold). The impact of the modifications on 5-HT_{1A} antagonist activity was quite drastic, with signicant losses with addition of the thioether linked ester (**6.1f**, 2.9-fold). The Boc-$dPEG_2$-linked material was nearly equal to alprenolol itself (**6.1a**, 0.64 μM), but the other versions were all completely inactive in the functional antagonist assays. The impact on β_2AR radioligand displacement was minimal (<5-fold) for all modifications except CCT (**6.1e**, 24.6-fold) and likewise for the functional antagonist IC50 except CCT (**6.1e**, 5.27-fold) consistent with the modifications being tolerated at β_2AR.

For alprenolol, there exists a second accessible vector for attaching the permeability modifiers by replacing the isopropyl amine group with alkyl linkers as had been done previously for making fluorescent alprenolol derivatives.[47] Based on published information, we used an extended $dPEG_4$ linker for this vector in order to maintain affinity at β_2AR. Synthesis of the modified derivatives was accomplished based on modification of published methods to give the desired products **6.2a-e**. Again, addition of the linker itself decreased PAMPA permeability to <0.1 x 10^{-6} cm/s for **6.2a-e**. 5-HT_{1A} binding of the $dPEG_4$-NHBoc and $dPEG_4$-NH_2 derivatives **6.2a-b** was unaffected (<2-fold) relative to **6**, but was more subtle with the permeability modifiers added (**6.2c**, 132-fold; **6.2d**, 12.1-fold; **6.2e**, 82.4-fold). In contrast, functional antagonist activity was drastically affected for all modifications tried, although alprenolol itself was only weakly active in this assay.
For β_2AR, the impact of permeability modifiers for the amine vector probes caused substantial loss of binding. The impact of alprenolol modification on β_2AR binding was modest for $dPEG_4$-NHBoc **6.2a** (7.4-fold), but quite extreme with the anionic groups added (**6.2c**, >1000-fold; **6.2d**, 150-fold; **6.2e**, >1000-fold), but given the extremely high affinity of **6** for β_2AR (0.5 nM) the dynamic range for β_2AR is far greater than for 5-HT_{1A} where alprenolol is weaker (**7**, 21.6 nM). Functional antagonist activity for β_2AR was impacted in a parallel manner (**6.2a**, 2-fold; **6.2b**, 30.3-fold; **6.2c**, 151-fold; **6.2d**, 25.3-fold and **6.2e**, >300-fold).

View Article Online
DOI: 10.1039/C9MD00412A

Table 2 (+)-JQ1 **1** and derivatives cLogP, PAMPA permeability, unbound drug accumulation ratio (Kp_{uu}), TR-FRET binding (BRD2, BRD3, BRD4) and cell-based data (MX-1 CellTiter-Glo, H1299 luciferase reporter assays).

			PAMPA[a]		TR-FRET IC_{50} (μM)[c]			Cell EC_{50} (μM)[d]			
Compnd	Modifier	cLogP	10^{-6} cm/s	Kp_{uu}[b]	BRD2	BRD3	BRD4	MX-1	Change[e]	H1299	Change[e]
(+)-JQ1, **1**	--	4.87	2.24	0.138	0.019	0.023	0.144	0.144	1	0.064	1
1a	Boc	4.15	6.22	0.168	0.035	0.042	0.526	0.526	3.65	0.718	11.2
1b	H	2.34	0.0146	0.0695	0.016	0.007	2.48	2.48	17.2	8.49	>50
1c	SCD	-2.96	NV	0.0064	>45	>20.5	9.11	9.11	>50	>10	>50
1d	SAA	-1.42	NV	0.0219	0.078	0.078	>10	>10	>50	>10	>50
1e	CCT	1.67	NV	0.0359	0.997	0.456	>10	>10	>50	>10	>50

[a]NV (no value) indicates no permeability detected. [b]Kp_{uu}, [c]TR-FRET IC_{50} and [d]Cell EC_{50} values are reported as the geometric mean from at least two duplicate runs. [e]Change indicates ratio of assay results relative to (+)-JQ1

Table 3 Olaparib **2** and derivatives cLogP, PAMPA permeability, TR-FRET binding (PARP1) and cell-based data (DLD wt, DLD *BRCA2*$^{-/-}$ CellTiter-Glo).

			PAMPA[a]	TR-FRET K_i (μM)[b]		Cell EC_{50} (μM)[c]		
Compnd	Modifier	cLogP	10^{-6} cm/s	PARP1	Change[d]	DLD (wt)	DLD (*BRCA*$^{-/-}$)	Change[d]
2	--	1.236	3.37	0.000787	1	19.0	0.10	1
2f	truncated	1.057	0.081	0.000376	0.48	>100	0.20	2
2a	Boc	2.123	NV	0.00192	2.43	>100	0.70	7
2b	H	0.315	0.00119	0.00148	1.88	>100	0.60	6
2c	SCD	-4.894	NV	0.00056	0.71	70.0	0.60	6
2d	SAA	-1.519	NV	0.0106	13.4	53.0	1.10	11
2e	CCT	-0.354	NV	0.0415	>50	>100	7.80	>50

[a]NV (no value) indicates indicates no permeability detected. [b]TR-FRET K_i and [c]Cell EC_{50} values are reported as the geometric mean from at least two duplicate runs. [d]Change indicates ratio of assay results to olaparib **2**

Table 4 Dasatinib **3** and derivatives cLogP, PAMPA permeability, unbound drug accumulation ratio (Kp_{uu}), TR-FRET binding (Abl, Src), and cell-viability data (K562 CellTiter-Glo).

			PAMPA[a]		TR-FRET K_i (nM)[c]				Cell IC_{50} (μM)[d]	
Compnd	Modifier	cLogP	10^{-6} cm/s	Kp_{uu}[b]	Abl	Change[e]	Src	Change[d]	K562	Change[e]
3	--	2.379	1.49	0.712	0.457	1	0.295	1	0.000638	1
3f	truncated	2.459	0.0371	0.654	3.30	7.2	0.449	1.52	NA[e]	NA[f]
3a	Boc	4.144	0.0065	0.0177	0.418	0.915	0.785	2.66	0.00164	2.57
3b	H	2.336	0.056	0.00055	0.103	0.225	0.261	0.88	0.62783	>50
3c	SCD	-5.143	NV	0.00606	0.35[g]	0.766	0.37[f]	1.25	0.02913	45.7
3d	SAA	-1.767	0.0274	0.0196	0.49	1.07	0.851	2.88	0.11976	>50
3e	CCT	-0.603	0.0122	0.397	0.507	1.11	0.925	3.14	0.18259	>50

[a]NV (no value) indicates indicates no permeability detected. [b]Kp_{uu}, [c]TR-FRET K_i and [d]Cell IC_{50} proliferation values reported as the geometric mean from at least two duplicate runs. [e]Change indicates ratio of assay results relative to dasatinib **3**. [f]NA (not available) indicates compound not tested in this assay. [g]SCD fluorescence interferes with TR-FRET assays, assay run with Eurofins DiscoverX Kinoscan

Table 5 NAMPT inhibitor **4** and derivatives cLogP, PAMPA permeability, TR-FRET binding , and cell-based data (PC3 CellTiter-Glo).

			PAMPA[a]	TR-FRET K_i (μM)[b]				Cell Viability IC_{50} (μM)[c]	
Compnd	Modifier	cLogP	10^{-6} cm/s	NAMPT[d] (-PRPP)	Change[e]	NAMPT[d] (+PRPP)	Change[e]	PC3	Change[e]
4	--	2.991	39.5	0.006	1	0.0002	1	0.0060	1
4f	CH_2-NH_2	1.943	0.092	0.055	9.2	0.0011	5.5	0.0302	5.0
4a	Boc	2.834	1.2	0.014	2.33	0.0002	1	0.0307	5.1
4b	H	1.030	0.016	0.060	10.0	0.0019	9.5	0.2963	49.5
4c	SCD	-4.18	NV	0.141	23.5	0.0013	6.5	0.1968	32.9
4d	SAA	-0.803	NV	0.285	47.5	0.0079	39.5	7.2252	>1000
4e	CCT	0.361	NV	0.359	59.8	0.0059	29.5	7.3261	>1000

[a]NV (no value) indicates indicates no permeability detected. [b]TR-FRET K_i and [c]Cell IC_{50} proliferation values reported as the geometric mean from at least two duplicate runs. [d]NAMPT (-PRPP), NAMPT (+PRPP) indicates the assay run without and with 200 μM 5-phosphoribosyl-1-pyrophosphate. [e]Change indicates ratio of assay results relative to dasatinib **4**.

View Article Online
DOI: 10.1039/C8MD00412A

Table 6 CLogP, CEREP H_3 receptor cell-based data for the H_3 receptor ligand **5** and derivatives.

Compnd	Mod.	cLogP	PAMPA[a] 10^{-6} cm/s	CEREP Human H_3 Assay Data[b]				
				Binding Antagonist K_i (μM)	Change[c]	Functional Antagonist IC50 (μM)	Change[c]	Functional Agonist EC50 (μM)
5	--	3.436	1.13	0.00045[d]	1	0.043	1	>3
5a	Boc	4.510	0.873	0.0015	33	0.041	0.95	>3
5b	H	2.702	0.0246	0.0007	1.6	0.001	0.02	>3
5c	SCD	-7.488	0.284	0.0019	4.2	0.013	0.3	0.088
5d	SAA	-1.402	NV	0.0056	12.4	0.045	1.0	>3
5e	CCT	-0.238	0.0131	0.0254	56	0.15	3.5	>3

[a]NV (no value) indicates indicates no permeability detected. [b]CEREP H_3 antagonist binding, functional antagonist and functional agonist assay results. [c]Change indicates ratio of assay results relative to **5**. [d]Binding affinity determined by published radioligand displacement assay.[51]

Table 7 CLogP, CEREP 5-HT_{1A} and β_2AR receptor cell-based binding data for alprenolol **6** derivatives based on thio-ene reaction.

Compnd	Modifier	cLogP	PAMPA[a] 10^{-6} cm/s	CEREP 5-HT_{1A}[b]				CEREP β_2AR[c]			
				K_i (μM)	Change[d]	Func. Antag. IC50 (μM)	Change[d]	K_i (μM)	Change[d]	Func. Antag. IC50 (μM)	Change[d]
6	--	2.652	10.9	0.0216	0.38	0.630	0.217	0.0005	0.033	0.0033	0.046
6.1f	SCH_2COOMe	2.431	0.0436	0.0561	1	2.900	1	0.015	1	0.072	1
6.1a	Boc	3.018	0.0189	0.0489	0.871	0.640	0.22	0.0032	0.21	0.022	0.31
6.1b	H	1.210	NV	0.3090	6.32	>10	>5	0.0029	0.19	0.019	0.26
6.1c	SCD	-6.269	NV	0.925	18.9	>10	>5	0.0260	1.73	0.096	1.33
6.1d	SAA	-2.893	NV	0.740	15.1	>10	>5	0.0164	1.09	0.086	1.19
6.1e	CCT	-1.729	0.0035	1.72	35.2	>10	>5	0.0786	24.6	0.380	5.27

[a]NV (no value) indicates indicates no permeability detected. [b]CEREP 5-HT_{1A} radioligand displacement assay and functional antagonist assays. [c]CEREP β_2AR radioligand displacement and functional antagonist assays. [d]Change indicates ratio of assay results relative to **6.1f**

Table 8 CLogP, CEREP 5-HT_{1A} and β_2AR receptor cell-based binding data for alprenolol **6** derivatives based on on epoxide opening reaction.

Compnd	Modifier	cLogP	PAMPA[a] 10^{-6} cm/s	CEREP 5-HT_{1A}[b]				CEREP β_2AR[c]			
				K_i (μM)	Change[d]	Func. Antag. IC50 (μM)	Change[d]	K_i (μM)	Change[d]	Func. Antag. IC50 (μM)	Change[d]
6	--	2.652	10.9	0.0216	1	0.630	1	0.0005	1	0.0033	1
6.2a	Boc	2.761	0.035	0.0241	1.12	>1	--	0.0037	7.4	0.0069	2.09
6.2b	H	0.954	0.032	0.0358	1.66	>1	--	0.0103	20.6	0.10	30.3
6.2c	SCD	-6.526	NV	2.86	132	>1	--	0.547	1094	0.50	151
6.2d	SAA	-3.150	0.0046	0.261	12.1	>1	--	0.752	150	0.0834	25.3
6.2e	CCT	-1.986	0.0012	1.78	82.4	>1	--	0.512	1024	>1	303

[a]NV (no value) indicates indicates no permeability detected. [b]CEREP 5-HT_{1A} radioligand displacement assay and functional antagonist assays. [c]CEREP β_2AR radioligand displacement and functional antagonist assays. [d]Change indicates ratio of assay results relative to **6**.

Conclusions

While originally conceived as a means to allow rapid binning of phenotypic screening hits into cell-surface and intracellular targets, the data from this extensive test set is more nuanced. Our test cases were all high-potency compounds for which there was SAR/structural data to drive the design of the intermediate $dPEG_2$-NHBoc and modified conjugates. For phenotypic assay hits with unknown targets this information may not be available so more substantial work in deriving linked intermediates may be necessary to maintain potency with such less optimized systems. In the cases here the activity of the $dPEG_2$-NHBoc derivatives was generally maintained regardless of subcellular localization of target(s), but for phenotypic assay hits that may not be the case. Secondarily, these results show that all the anionic permeability modifiers are able to effectively prevent

engagement of intracellular targets, with the small sulfonic acid (SAA) and polycarboxylic acid (CCT) being most consistent, whereas the polysulfonic fluorophore (SCD) impacts permeability independent direct target binding, as well as causing interference in fluorescence-based assays (dasatinib TR-FRET). The effect of the modifications on the biophysical unbound drug accumulation (Kp_{uu}) values matched the biological results for the subset of targets tested (Brd, dasatinib, H_3 receptor), though the relevance for cell-surface targets is unclear. For cell-surface targets (H_3, 5-HT_{1A}, β_2AR) binding potency, and functional activity was impacted by the modifiers to such an extent that it would not be possible to conclude that loss of activity with modifier addition means the target is intracellular. However, we can conclude that if addition of one of these anionic modifiers maintains cellular activity, the target is very likely cell-surface. The impact on agonist compounds for cell-surface targets was not a topic covered in this work. Future work in this area will explore the effect of permeability modifiers on compounds known to act on transporters or are uptaken by endo/pinocytosis as that could complicate interpretation of the results. In addition, direct comparison to macromolecular conjugates used for controlling cellular uptake will be explored.

Experimental

Synthesis of linked and linked permeability modified compounds

Detailed synthetic procedures and characterization of all newly described compounds in the supplementary material.

Physicochemical property determinations

Calculated n-octanol/water partition coefficients (cLogP) were determined using ChemDraw Professional™.

Bromodomain TR-FRET binding and cell-based assays

TR-FRET binding assays for BRD2, BRD3 and BRD4; MX-1 Cell-Titer Glo proliferation, and H1299-luciferase reporter assays were run as previously described (Table 2).[22]

PARP1 TR-FRET binding and cell-based assays

TR-FRET binding assays for PARP1; CellTiter-Glo cell-viability assays [DLD (wt), and DLD (*BRCA*$^{-/-}$)] were run as previously described (Table 3).[25]

Kinase TR-FRET assays

TR-FRET binding assays for primary (Abl, Src; Table 4) and secondary targets (Table S1, Figure S1) were run as previously described.[28]

Dasatinib analog cell viability assays

K562 cells from ATCC were cultured in RPMI 1640 containing 50 mM HEPES (Gibco 22400) supplemented with 10% fetal bovine serum at 37 °C in 5% CO_2/80% relative humidity, then plated 20,000 cells/well in 96-well white plates (Corning 3610) in 90 µL of growth media. Compounds were serially diluted in log increments in DMSO from 10,000 µM to 0.01 µM, and then further diluted 100X in RPMI media. Addition of 10 µL of the compound solution to the cell wells resulted in final compound concentrations of 10,000 nM to 0.01 nM. Cell plates were incubated with compound for 3 days and cell viability determined using CellTiter-Glo viability assay detection of total intracellular ATP.

NAMPT TR-FRET binding and cell-based assays

Equilibrium TR-FRET binding assays measuring displacement of a fluorescent OG488-labeled version of compound **4b** was run essentially as described.[50] CellTiter-Glo viability assays (PC3 cell-line, originally from ATCC and authenticated by STR analysis) were run as previously described (Table 5).[43]

Intracellular compound binding and accumulation

Unbound compound accumulation ratios (Kp_{uu}) consisting of compound binding ($f_{u,\,HEK}$) and intracellular accumulation (Kp) was determined in HEK293 cells (from ATCC) similar to previously described methods.[16] Modifications to the referenced method and details on the analytical methods can be found in the supplementary material under Detailed Analytical Methods.

Acknowledgements

We thank Michael Curtin for providing the NAMPT compound 4f; Anita McGreal and Frank Wagenaar for assistance with compound purification; Gilbert Diaz for coordinating CEREP screening; and Henning Stöckmann for critical advice and editing on the manuscript; Rick Yarbrough, Jan Waters, David Whittern and Ian Marsden for assistance in interpretation of NMR spectra.

Disclaimers

All authors are employees of AbbVie. The design, study conduct, and financial support for this research were provided by AbbVie. AbbVie participated in the interpretation of data, review and approval of this publication.

Notes and references

1 A. DiMasi Joseph, G. Grabowski Henry and W. Hansen Ronald, *Journal of health economics*, 2016, **47**, 20-33.
2 D. C. Swinney, *Clinical Pharmacology & Therapeutics (New York, NY, United States)*, 2013, **93**, 299-301.

3 L. H. Jones and M. E. Bunnage, *Nature Reviews Drug Discovery*, 2017, **16**, 285-296.

4 J. G. Moffat, F. Vincent, J. A. Lee, J. Eder and M. Prunotto, *Nature Reviews Drug Discovery*, 2017, **16**, 531-543.

5 M. Kawatani and H. Osada, *MedChemComm*, 2014, **5**, 277-287.

6 M. J.. Niphakis, K.M. Lum, A.B. Cognetta, B. E. Correia, T. A Ichu, J. Olucha, S. J. Brown, S. Kundu, F. Piscitelli, H. Rosen, B. F. Cravatt, *Cell*, 2015, **161**, 1668-1680.

7 D. P. Murale, S. C. Hong, M. M. Haque, J.-S. Lee, *Proteome Science*, 2017, **15**, 1-34

8 H. Tang, S. Duggan, P. L. Richardson, V. Marin, S. E. Warder and S. M. McLoughlin, *Journal of Biomolecular Screening*, 2016, **21**, 201-211.

9 S.-h. Fujishima, R. Yasui, T. Miki, A. Ojida and I. Hamachi, *Journal of the American Chemical Society*, 2012, **134**, 3961-3964.

10 H. Stockmann, V. Todorovic, P. L. Richardson, V. Marin, V. Scott, C. Gerstein, M. Lake, L. Wang, R. Sadhukhan and A. Vasudevan, *Journal of the American Chemical Society*, 2017, **139**, 16822-16829.

11 S. Vernocchi, N. Battello, S. Schmitz, D. Revets, A. M. Billing, J. D. Turner and C. P. Muller, *Molecular & Cellular Proteomics*, 2013, **12**, 1764-1779.

12 J. A. Johnson, A. Olson, P. Dussault and R. Moreau, *Abstracts of Papers, 247th ACS National Meeting & Exposition, Dallas, TX, United States, March 16-20, 2014*, 2014, CHED-995.

13 H. Abe, K. L. Keen and E. Terasawa, *Endocrinology*, 2008, **149**, 1155-1162.

14 E. L. Rickert, S. Oriana, C. Hartman-Frey, X. Long, T. T. Webb, K. P. Nephew and R. V. Weatherman, *Bioconjugate Chemistry*, 2010, **21**, 903-910.

15 K. Kim, J. A. Kim, S.-G. Lee and W. G. Lee, *Nanoscale*, 2012, **4**, 5051-5058.

16 A. Mateus, P. Matsson, P, Artursson, *Molecular Pharmaceutics*, 2013, **10**, 2467-2478.

17 G. Ottaviani, S. Martel and P.-A. Carrupt, *Journal of Medicinal Chemistry*, 2006, **49**, 3948-3954.

18 H. Gursahani, J. Riggs-Sauthier, J. Pfeiffer, D. Lechuga-Ballesteros and C. S. Fishburn, *Journal of Pharmaceutical Sciences*, 2009, **98**, 2847-2856.

19 S. Miyoshi, S. Ooike, K. Iwata, H. Hikawa, K. Sugahara, Mitsubishi Tanabe Pharma, JP Pat., 2008-JP73864, WO2009084693.

20 P. Filippakopoulos, J. Qi, S. Picaud, Y. Shen, W. B. Smith, O. Fedorov, E. M. Morse, T. Keates, T. T. Hickman, I. Felletar, M. Philpott, S. Munro, M. R. McKeown, Y. Wang, A. L. Christie, N. West, M. J. Cameron, B. Schwartz, T. D. Heightman, N. La Thangue, C. French, O. Wiest, A. L. Kung, S. Knapp and J. E. Bradner, *Nature (London, United Kingdom)*, 2010, **468**, 1067-1073.

21 L. Anders, M. G. Guenther, J. Qi, Z. P. Fan, J. J. Marineau, P. B. Rahl, J. Loven, A. A. Sigova, W. B. Smith, T. I. Lee, J. E. Bradner and R. A. Young, *Nature Biotechnology*, 2014, **32**, 92-96.

22 L. A. Hasvold, G. S. Sheppard, L. Wang, S. D. Fidanze, D. Liu, J. K. Pratt, R. A. Mantei, C. K. Wada, R. Hubbard, Y. Shen, X. Lin, X. Huang, S. E. Warder, D. Wilcox, L. Li, F. G. Buchanan, L. Smithee, D. H. Albert, T. J. Magoc, C. H. Park, A. M. Petros, S. C. Panchal, C. Sun, P. Kovar, N. B. Soni, S. W. Elmore, W. M. Kati and K. F. McDaniel, *Bioorganic & Medicinal Chemistry Letters*, 2017, **27**, 2225-2233.

23 K. A. Menear, C. Adcock, R. Boulter, X.-l. Cockcroft, L. Copsey, A. Cranston, K. J. Dillon, J. Drzewiecki, S. Garman, S. Gomez, H. Javaid, F. Kerrigan, C. Knights, A. Lau, V. M. Loh, Jr., I. T. W. Matthews, S. Moore, M. J. O'Connor, G. C. M. Smith and N. M. B. Martin, *Journal of Medicinal Chemistry*, 2008, **51**, 6581-6591.

24 J. M. Dubach, C. Vinegoni, R. Mazitschek, P. Fumene Feruglio, L. A. Cameron and R. Weissleder, *Nature Communications*, 2014, **5**, 3946.

25 T. A. Hopkins, Y. Shi, L. E. Rodriguez, L. R. Solomon, C. K. Donawho, E. L. DiGiammarino, S. C. Panchal, J. L. Wilsbacher, W. Gao, A. M. Olson, D. F. Stolarik, D. J. Osterling, E. F. Johnson and D. Maag, *Molecular Cancer Research*, 2015, **13**, 1465-1477.

26 M. Talpaz, N. P. Shah, H. Kantarjian, N. Donato, J. Nicoll, R. Paquette, J. Cortes, S. O'Brien, C. Nicaise, E. Bleickardt, M. A. Blackwood-Chirchir, V. Iyer, T.-T. Chen, F. Huang, A. P. Decillis and C. L. Sawyers, *New England Journal of Medicine*, 2006, **354**, 2531-2541.

27 H. Shi, C.-J. Zhang, G. Y. J. Chen and S. Q. Yao, *Journal of the American Chemical Society*, 2012, **134**, 3001-3014.

28 W. Karaman Mazen, S. Herrgard, K. Treiber Daniel, P. Gallant, E. Atteridge Corey, T. Campbell Brian, W. Chan Katrina, P. Ciceri, I. Davis Mindy, T. Edeen Philip, R. Faraoni, M. Floyd, P. Hunt Jeremy, J. Lockhart Daniel, V. Milanov Zdravko, J. Morrison Michael, G. Pallares, K. Patel Hitesh, S. Pritchard, M. Wodicka Lisa and P. Zarrinkar Patrick, *Nat Biotechnol*, 2008, **26**, 127-132.

29 J. Marjanovic, A. Baranczak, V. Marin, H. Stockmann, P. L. Richardson and A. Vasudevan, *MedChemComm*, 2017, **8**, 789-795.

30 D. R. Veach, M. Namavari, N. Pillarsetty, E. B. Santos, T. Beresten-Kochetkov, C. Lambek, B. J. Punzalan, C. Antczak, P. M. Smith-Jones, H. Djaballah, B. Clarkson and S. M. Larson, *Journal of Medicinal Chemistry*, 2007, **50**, 5853-5857.

31 E. R. Goedken, M. A. Argiriadi, D. L. Banach, B. A. Fiamengo, S. E. Foley, K. E. Frank, J. S. George, C. M. Harris, A. D. Hobson, D. C. Ihle, D. Marcotte, P. J. Merta, M. E. Michalak, S. E. Murdock, M. J. Tomlinson and J. W. Voss, *Journal of Biological Chemistry*, 2015, **290**, 4573-4589.

32 S. Lebakken Connie, M. Riddle Steven, U. Singh, W. J. Frazee, C. Eliason Hildegard, Y. Gao, J. Reichling Laurie, D. Marks Bryan and W. Vogel Kurt, *J Biomol Screen*, 2009, **14**, 924-935.

33 M. A. Fabian, W. H. Biggs, D. K. Treiber, C. E. Atteridge, M. D. Azimioara, M. G. Benedetti, T. A. Carter, P. Ciceri, P. T. Edeen, M. Floyd, J. M. Ford, M. Galvin, J. L. Gerlach, R. M. Grotzfeld, S. Herrgard, D. E. Insko, M. A. Insko, A. G. Lai, J.-M. Lelias, S. A. Mehta, Z. V. Milanov, A. M. Velasco, L. M.

Wodicka, H. K. Patel, P. P. Zarrinkar and D. J. Lockhart, *Nature Biotechnology*, 2005, **23**, 329-336.

34 M. W. Karaman, S. Herrgard, D. K. Treiber, P. Gallant, C. E. Atteridge, B. T. Campbell, K. W. Chan, P. Ciceri, M. I. Davis, P. T. Edeen, R. Faraoni, M. Floyd, J. P. Hunt, D. J. Lockhart, Z. V. Milanov, M. J. Morrison, G. Pallares, H. K. Patel, S. Pritchard, L. M. Wodicka and P. P. Zarrinkar, *Nature Biotechnology*, 2008, **26**, 127-132.

35 S.-C. Mei and C. Brenner, *Chemistry & Biology (Oxford, United Kingdom)*, 2013, **20**, 1307-1308.

36 A. Roulston and G. C. Shore, *Molecular & Cellular Oncology*, 2016, **3**, e1052180/1052181-e1052180/1052112.

37 M. L. Curtin, H. R. Heyman, R. F. Clark, B. K. Sorensen, G. A. Doherty, T. M. Hansen, R. R. Frey, K. A. Sarris, A. L. Aguirre, A. Shrestha, N. Tu, K. Woller, M. A. Pliushchev, R. F. Sweis, M. Cheng, J. L. Wilsbacher, P. J. Kovar, J. Guo, D. Cheng, K. L. Longenecker, D. Raich, A. V. Korepanova, N. B. Soni, M. A. Algire, P. L. Richardson, V. L. Marin, I. Badagnani, A. Vasudevan, F. G. Buchanan, D. Maag, G. G. Chiang, C. Tse and M. R. Michaelides, *Bioorganic & Medicinal Chemistry Letters*, 2017, **27**, 3317-3325.

38 U. Galli, E. Ercolano, L. Carraro, C. R. B. Roman, G. Sorba, P. L. Canonico, A. A. Genazzani, G. C. Tron and R. A. Billington, *ChemMedChem*, 2008, **3**, 771-779.

39 E. Biedermann, M. Hasmann, R. Loser, B. Rattel, F. Reiter, B. Schein, K. Seibel, K. Vogt, Klinge Pharma GMBH, WO9748696A1, 1997.

40 J. L. Wilsbacher, M. Cheng, D. Cheng, S. A. J. Trammell, Y. Shi, J. Guo, S. L. Koeniger, P. J. Kovar, Y. He, S. Selvaraju, H. R. Heyman, B. K. Sorensen, R. F. Clark, T. M. Hansen, K. L. Longenecker, D. Raich, A. V. Korepanova, S. Cepa, D. L. Towne, V. C. Abraham, H. Tang, P. L. Richardson, S. M. McLoughlin, I. Badagnani, M. L. Curtin, M. R. Michaelides, D. Maag, F. G. Buchanan, G. G. Chiang, W. Gao, S. H. Rosenberg, C. Brenner and C. Tse, *Molecular Cancer Therapeutics*, 2017, **16**, 1236-1245.

41 M. E. Parsons and C. R. Ganellin, *British Journal of Pharmacology*, 2006, **147**, S127-S135.

42 S. J. Hill, C. R. Ganellin, H. Timmerman, J. C. Schwartz, N. P. Shankley, J. M. Young, W. Schunack, R. Levi and H. L. Haas, *Pharmacological reviews*, 1997, **49**, 253-278.

43 R. J. Altenbach, H. Liu, P. N. Banfor, K. E. Browman, G. B. Fox, R. M. Fryer, V. A. Komater, K. M. Krueger, K. Marsh, T. R. Miller, J. B. Pan, L. Pan, M. Sun, C. Thiffault, J. Wetter, C. Zhao, D. Zhou, T. A. Esbenshade, A. A. Hancock and M. D. Cowart, *Journal of Medicinal Chemistry*, 2007, **50**, 5439-5448.

44 A. Brandstrom, H. Corrodi, U. Junggren and T. E. Jonsson, *Acta Pharmaceutica Suecica*, 1966, **3**, 303-310.

45 M. Langlois, B. Bremont, D. Rousselle and F. Gaudy, *European Journal of Pharmacology, Molecular Pharmacology Section*, 1993, **244**, 77-87.

46 M. G. Caron, Y. Srinivasan, J. Pitha, K. Kociolek and R. J. Lefkowitz, *Journal of Biological Chemistry*, 1979, **254**, 2923-2927.

47 J. G. Baker, L. A. Adams, K. Salchow, S. N. Mistry, R. J. Middleton, S. J. Hill and B. Kellam, *Journal of Medicinal Chemistry*, 2011, **54**, 6874-6887.

48 M. H. Keylor, J. E. Park, C.-J. Wallentin and C. R. J. Stephenson, *Tetrahedron*, 2014, **70**, 4264-4269.

49 A. Vasudevan, C. Villamil, J. Trumbull, J. Olson, D. Sutherland, J. Pan and S. Djuric, *Tetrahedron Letters*, 2010, **51**, 4007-4009.

50 L. Curtin Michael, H. R. Heyman, F. Clark Richard, K. Sorensen Bryan, A. Doherty George, T. M. Hansen, R. Frey Robin, A. Sarris Kathy, L. Aguirre Ana, A. Shrestha, N. Tu, K. Woller, A. Pliushchev Marina, F. Sweis Ramzi, M. Cheng, L. Wilsbacher Julie, J. Kovar Peter, J. Guo, D. Cheng, L. Longenecker Kenton, D. Raich, V. Korepanova Alla, B. Soni Nirupama, A. Algire Mikkel, L. Richardson Paul, L. Marin Violeta, I. Badagnani, A. Vasudevan, F. G. Buchanan, D. Maag, G. Chiang Gary, C. Tse and R. Michaelides Michael, *Bioorg Med Chem Lett*, 2017, **27**, 3317-3325.

51 H. Liu, R. J. Altenbach, G. J. Diaz, A. M. Manelli, R. L. Martin, T. R. Miller, T. A. Esbenshade, J. D. Brioni, M. D. Cowart, *Bioorg Med Chem Lett*, 2010, **20**, 3295-3300.

View Article Online
DOI: 10.1039/C8MD00412A

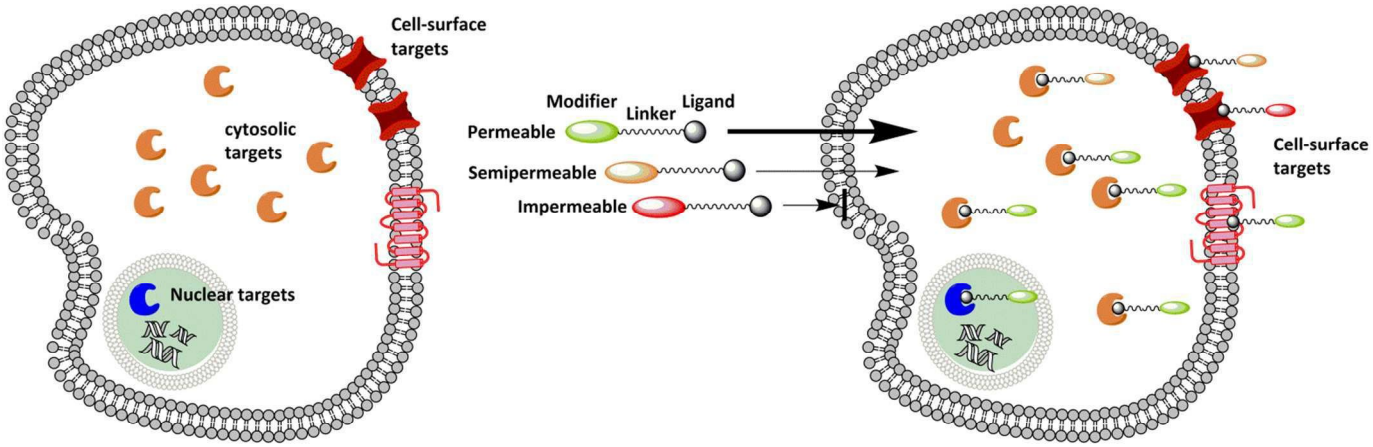

Fig. 1 General strategy for permeability modified ligands. Nuclear and cytosolic targets are only accessible with permeable/semi-permeable modifiers. Cell-surface targets are accessable by all modification forms.

View Article Online
DOI: 10.1039/C8MD00412A

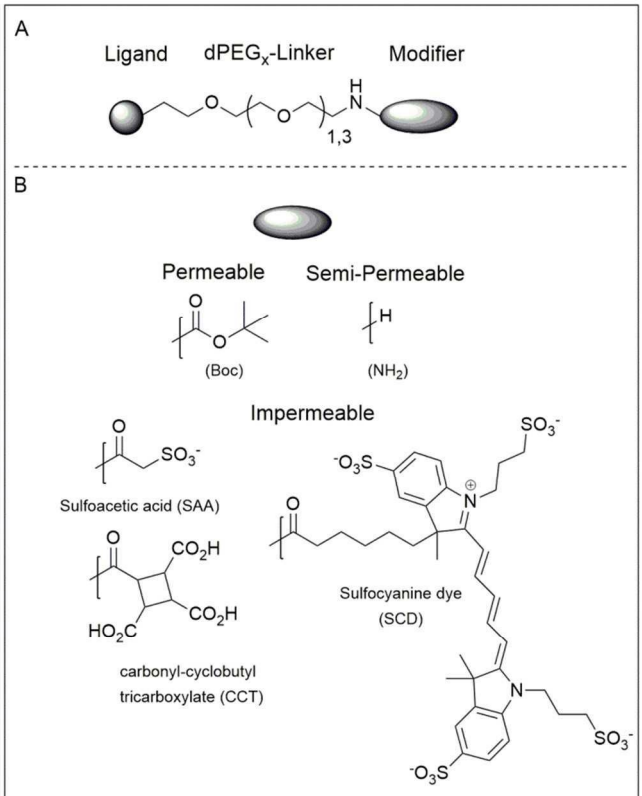

Fig. 2 (A) General design of permeability-modified probes with dPEG$_x$-linker (B) Structures of specific permebility modifiers added to linked ligands.

View Article Online
DOI: 10.1039/C8MD00412A

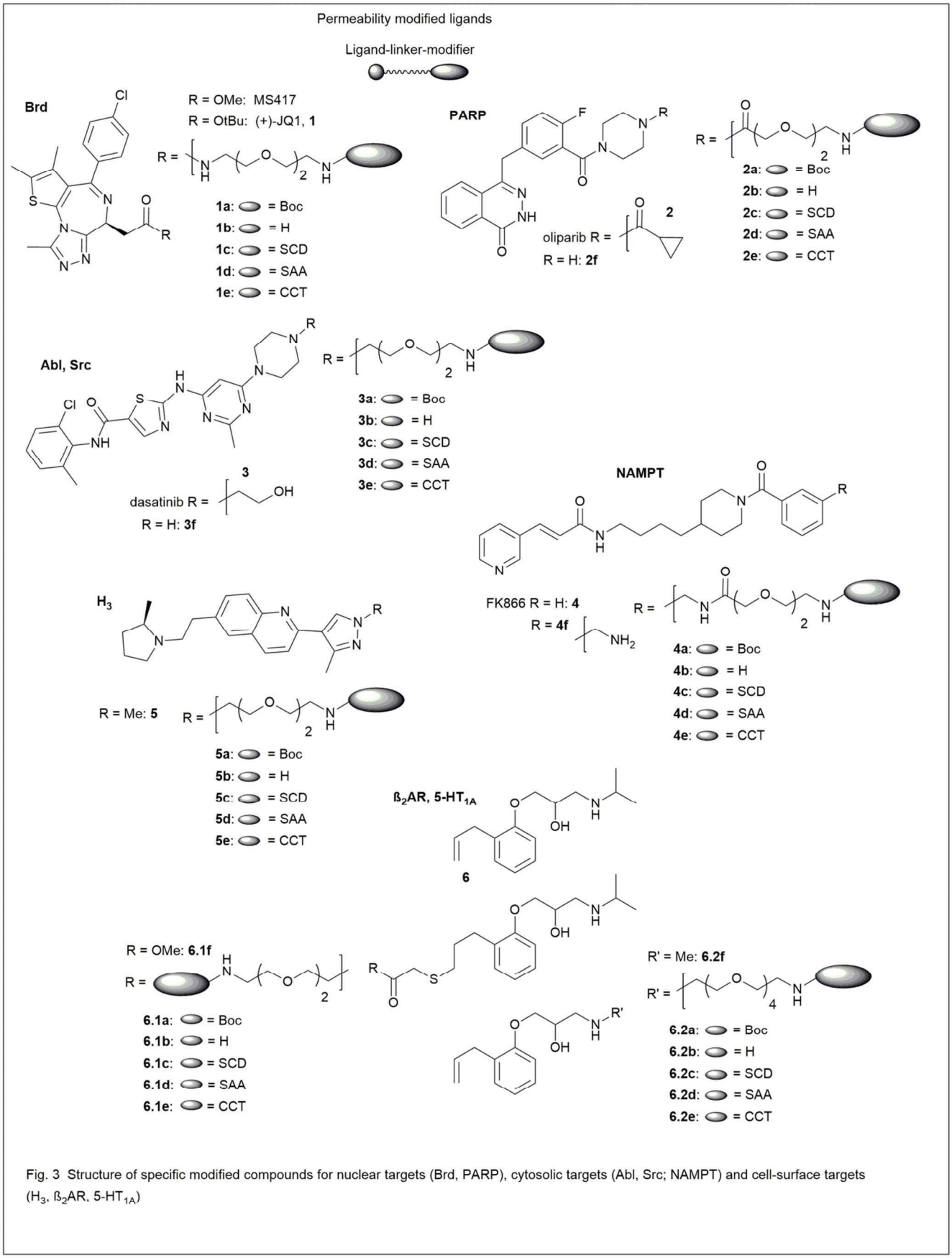

Fig. 3 Structure of specific modified compounds for nuclear targets (Brd, PARP), cytosolic targets (Abl, Src; NAMPT) and cell-surface targets (H_3, $ß_2$AR, 5-HT_{1A})

View Article Online
DOI: 10.1039/C8MD00412A

Controlling Cellular Distribution of Drugs with Permeability Modifying Moieties

Paul L. Richardson,*[a] Violeta L. Marin,[a] Stormy L. Koeniger,[a] Aleksandra Baranczak,[a] Julie L. Wilsbacher,[b] Peter J. Kovar,[b] Patricia E. Bacon-Trusk,[b] Min Cheng,[b] Todd A. Hopkins,[b] Sandra T. Haman,[b] and Anil Vasudevan[a]

Anionic moieties can be used to control the cell-permeability of drugs and used to select the appropriate target identification method for phenotypic screening hits.